Supplement of

Sustained Late-Nineteenth-Century Monsoon Drought in Seoul and the Indian Ocean–North Atlantic Forcing of Its Circulation Weakening

Byung-Kwon Moon

Division of Science Education and Institute of Fusion Science, Jeonbuk National University, Jeonju, 54896, Republic of Korea

Contents of this file

- Text S1 to S7
- Figures S1 to S4
- Tables S1 to S5

Introduction

This Supplement documents (S1) the reconciliation of the two Cheugugi reconstructions and their adjudication against the original Seungjeongwon Ilgi gauge entries; (S2) robustness of the drought and its change point; (S3) record-integrity test that argues against decayed observational practice; (S4) intraseasonal variance decomposition that rules out a change in monsoon intraseasonal variability; (S5) design of the SST-forced attribution experiments and their basin-by-basin circulation response; (S6) moisture-flux diagnostic linking the circulation weakening to the moisture supply; and (S7) linearity of the basin decomposition. Tables S1–S5 and Figs. S1–S4 support these analyses.

Text S1. Reconciliation and adjudication against original chronicle

The reconstruction of Jhun and Moon (1997; hereafter J-Data) and the independent documentary reconstruction of Lee et al. (2024; R-Data), both derived from the Joseon royal chronicles, agree closely at the annual resolution (r = 0.97) but differ on individual days. We identified every substantive discrepancy — both multi-day events [difference exceeding maximum (6 mm, 30% of the larger total), or presence in one series and absence in the other] and single-day value disagreements [difference exceeding maximum (4 mm, 20%) after accounting for 1 d attribution shifts] — 732 in total, spanning 1,001 individual adjudicated days (multi-day events contribute several days each). For each, we retrieved the corresponding entries of the Seungjeongwon Ilgi from the National Institute of Korean History (NIKH) database (sjw.history.go.kr), converting Gregorian dates to the Joseon lunisolar calendar. The chronicle records rainfall as gauge water depth in the traditional units 尺 (chuk), 寸 (chon), and 分 (pun), with 1 尺 = 10 寸 = 100 分 and 1 分 = 2 mm; a typical entry reads 測雨器水深〇尺〇寸〇分. The values were automatically parsed.

The reconciled dataset (Cheugugi-Seoul v2) adopts the NIKH database value as the amount reference. Of the adjudicated discrepancies, 304 d resolved to a database value corroborated by one or both reconstructions; the remainder (697 d) were flagged for manual source review and carried provisional values (the database value where available, otherwise the Jhun–Moon value), of which 69 high-impact days (the highest-amount discrepancies) were listed with source links in the released dataset for completion. The drought was insensitive to these provisional days: setting all 697 to their maximum candidate value — the most anti-drought choice possible — changes the epoch contrast only from 1251→904 mm (−28%) to 1293→972 mm (−25%). Individual extreme days showed that discrepancies have two distinct origins. Some are transcription differences: on 16 July 1885, the database recorded 一尺四寸六分 (292 mm), matching R-Data, resolved to 292 mm in v2. Others relate to day-attribution differences for rainfall that spanned midnight: on 19 July 1832, the gauge record ran from

06h to 30h (i.e., until 06h of the following day), logged as 348.5 mm on the onset day by J-Data but 286 mm by the single-day database entry — not an error but a boundary choice, preserved in v2 through the recorded onset and end times. The multidecadal drought was unchanged under the reconciliation (1251 versus 904 mm across the epoch). Table S1 gives the resulting per-day provenance classification of the full 1777–1907 series. The first year (1777) is incompletely recorded — the monsoon-peak month of July was blank and only 32 wet days appeared, against 44–71 in 1778–1789 — and was excluded from the epoch statistics, which begin in 1778; later years showed no comparable deficiency.

Table S1: Per-day provenance classification of reconciled series (Cheugugi-Seoul v2).

Provenance class	Amount adopted	Flag	Days
Sources agree (J-Data = R-Data)	Jhun–Moon (= R-Data)	reference	38,079
Pre-1801, single source (Jeongjo era)	Jhun–Moon	reference	8,765
NIKH database corroborates both	database (= J = R)	reference	125
NIKH database supports Jhun–Moon	database (= J)	reference	68
NIKH database supports Lee et al.	database (= R)	reference	111
No gauge entry in chronicle	Jhun–Moon	manual review	485
NIKH database differs from both	database	manual review	212
Total			**47,845**

The 697 d flagged for manual review (last two classes) carry provisional values, of which 69 high-impact days are listed with source links in the released dataset; the drought was insensitive to their treatment (Text S1). Days marked "reference" take the amount directly from the source shown, with the NIKH original chronicle as the adjudicating authority. Pre-1801 (Jeongjo-era) days are carried from the Jhun–Moon restoration alone, since the day-level reconciliation with R-Data was performed from 1801 onward.

Text S2. Robustness of the drought and its change point

The 1881–1907 epoch was the driest 27-year window in the entire 1777–1907 record: based on the 27-year running mean, it ranked first of 105 overlapping windows for both annual (904 mm) and rainy-season (June–August; 580 mm) totals, against a record maximum of 1393 mm (annual; 1809–1835). The difference between the 1778–1880 and 1881–1907 annual means (1251 versus 904 mm) was significant (Student's t-test, $p = 3.3 \times 10^{-5}$; non-parametric Mann–Whitney U test, $p = 1.1 \times 10^{-4}$; 20,000-sample permutation test, $p = 1 \times 10^{-4}$); a 5-year moving-block bootstrap places the 95% confidence interval of the difference at [216, 478] mm, excluding zero. These epoch tests were evaluated at the data-selected change point and therefore represent the effect size rather than independent significance; the search-corrected Pettitt value ($p \approx 0.01$) was adopted as the headline significance. Because year-to-year autocorrelation was negligible (lag-1 $r = 0.10$), serial dependence does not inflate these significances. Perturbing the annual series by observational noise (15% of its standard deviation) and re-detecting the Pettitt change point yielded a 90% interval of [1879, 1881] (median 1880), indicating the change point is well constrained.

Text S3. Exclusion of observational-practice decay

Because the drought coincided with the final decades of the dynasty, we tested whether reduced gauge reading, rather than reduced rainfall, could produce the drought signal. Three lines of evidence exclude this possibility. First, the number of days on which the Seungjeongwon Ilgi qualitatively reports rain — an entirely separate textual channel from the quantitative gauge measurement — declined with its own Pettitt change point in 1881 ($p < 10^{-4}$), tracking the measured wet-day counts of both reconstructions (Fig. 1d of the main text). Had the gauge merely been read less often, qualitative rain reports would have persisted. Second, the ratio of measured to reported rain days remained stable through 1901 and spiked only in 1902–1904 (Fig. S2), indicating that any late-dynasty record degradation occurred in the qualitative diary channel and after the drought onset, not in the gauge series during it. Third, the precipitation amount attributable to any plausible under-counting of light rain was ~0.1 mm yr^{-1}, more than three orders of magnitude smaller than the observed rainy-season (JJA) deficit of ~217 mm yr^{-1}.

Text S4. Intraseasonal variance decomposition

To test whether the drought reflects a reorganization of monsoon intraseasonal variability (for example, a change in the boreal-summer intraseasonal oscillation), we removed the smoothed daily climatology from the daily series and band-pass filtered the May–September anomalies (third-order Butterworth; the extended May–September season is retained because the 30–60 d band cannot be resolved within the 92-day JJA window) into synoptic (3–10 d), quasi-biweekly (10–20 d), and intraseasonal (30–60 d) bands, computing each year's variance in each band. Between epochs, variance declined in all bands roughly in proportion to the total (Table S2): the 30–60 d band fell 29% but its fraction of total variance was statistically indistinguishable between epochs ($p > 0.7$), as were the other bands. Therefore, the drought represented a broadband reduction of rainfall variability consistent with reduced moisture supply, not a selective change in a particular intraseasonal mode.

Table S2: Extended-season (May–September) rainfall variance by frequency band.

Band	1778–1880 (mm^2)	1881–1907 (mm^2)	Change	*t*-test *p*-value
Total variance	327.8	262.8	−20%	0.22
Synoptic (3–10 d)	140.0	113.0	−19%	0.24
Quasi-biweekly (10–20 d)	37.6	32.9	−13%	0.45
Intraseasonal (30–60 d)	18.3	12.9	−29%	0.24

The intraseasonal (30–60 d) fraction of total variance is statistically indistinguishable between the two epochs (p > 0.7), confirming no selective change in that band.

Text S5. SST-forced attribution experiments

We attributed the oceanic driver of the circulation weakening accompanying the drought through prescribed-SST ("pacemaker") experiments using the atmospheric component of the JBNU Earth System Model, a spectral atmospheric general circulation model that originated as the CCSR/NIES AGCM5 (Numaguti et al., 1997) and was subsequently developed at Seoul National University into the SNU AGCM, including an improved parameterization of land-surface processes (Kim, 1999). The model employs a spectral dynamical core at T42 horizontal resolution (128 × 64 Gaussian grid, ~2.8°) with 20 σ-levels and a model top near 20 hPa; the low top truncates the middle stratosphere but does not affect the lower-tropospheric monsoon diagnostics on which the attribution rests (the 850 hPa circulation and the moisture flux integrated over 1000–300 hPa). Five experiments were conducted over 1854–1920: a control (CTL) forced by the model's monthly SST climatology, and four in which the observed ERSSTv5 monthly SST anomaly (relative to its own 1854–1920 mean) was added to the model's monthly climatology within a tanh-tapered regional mask covering the tropical Pacific (TP), North Atlantic (NA), Indian Ocean (IO), or global ocean (GOGA); the prescribed anomaly fields are shown in Fig. S4. Anomalies were tapered to zero under the sea-ice margin and clipped at the freezing point for consistency with the prescribed ice climatology, so that only the open-ocean SST differed between an anomaly and CTL experiment. Each experiment had 10 members that differed solely by a one-day-staggered start date. Because the boundary SST is linearly interpolated in time, this shift seeds independent internal-variability trajectories under identical forcing: the inter-member spread grew over the first few years and then saturated, thus the members decorrelate and sample independent internal variability. In four of the five experiments, a single member developed a transient single-step numerical instability during the integration; each was discarded and replaced by a member with a different start date, so that every experiment retained 10 completed members.

For each member and field, we determined the boreal-summer (JJA) drought-minus-baseline difference (1881–1907 minus 1855–1880). The SST-forced response was calculated as this difference in an anomaly experiment minus that in CTL, thus the CTL epoch change is an internal-variability null. Significance was determined using a two-sample Welch's *t*-test between the 10-member experiment and control groups. We diagnosed the low-level (850 hPa) circulation over the Korea box (34–43°N, 124–130°E) rather than local precipitation: the model's summer rain band lay ~7° too far south, so that the control rainfall was only 3.9 mm d^{-1} against 7.2 mm d^{-1} in GPCP (Adler et al., 2018), where Seoul sits on the dry northern flank, whereas the control 850 hPa monsoon circulation matched the NCEP reanalysis (Kalnay et al., 1996; western North Pacific monsoon index +4.1 versus +3.6 m s^{-1}). The forced response over the Korea box is summarized in Table S3.

Table S3: SST-forced 850 hPa circulation response over the Korea box (34–43°N, 124–130°E), JJA.

Forcing (exp − CTL)	Z850 (m)	*t*	*p*	V850 (m s^{-1})	*t*
Tropical Pacific (TP)	−1.8	−1.2	n.s.	−0.20	−2.1
North Atlantic (NA)	−3.7	−2.6	< 0.05	−0.20	−1.3
Indian Ocean (IO)	−5.0	−3.2	< 0.01	−0.09	−0.8
Global (GOGA)	−7.7	−5.8	< 0.001	−0.35	−2.5

The Indian Ocean is the largest single-basin contributor to the circulation weakening and the tropical Pacific the smallest; only the global (GOGA) and IO forcings are significant (p < 0.01). The single-basin Z850 responses are sub-additive (TP + NA + IO = −10.5 m versus GOGA −7.7 m), indicating saturation, though the residual (GOGA − sum) is not statistically significant (Text S7). Forced precipitation over the Korea box is weak for all experiments (and negligible for IO), reflecting the southward-displaced rain band, thus the attribution rests on the circulation. n.s., non-significant.

Text S6. Moisture-flux diagnostic (physical chain)

To link the circulation weakening to the moisture supply, we computed the vertically integrated moisture flux (VIMF = $g^{-1}\int qV\,dp$, integrated 1000–300 hPa; specific humidity, q; horizontal wind, V), and its convergence $-\nabla\cdot$VIMF, and determined the same JJA drought-minus-baseline and experiment-minus-control response as for the circulation (Table S4; Fig. 6 of the main text). Under the full forcing, the vertically integrated southerly (meridional) moisture flux into the Korea box weakened (−17.5 kg m^{-1} s^{-1}, $p < 0.05$), directly linking the circulation weakening to a reduced moisture supply; the moisture-flux convergence was negative (drying) for every forcing but, being a second derivative of the flux, was noisier and not individually significant.

Table S4: Forced vertically integrated moisture-flux response over the Korea box (34–43°N, 124–130°E), JJA (10-member ensembles; experiment − CTL).

Forcing (exp − CTL)	VIMFy (kg m^{-1} s^{-1})	*t*	MFC (mm d^{-1})	*t*
Tropical Pacific (TP)	−9.4	−2.0	−0.32	−1.4
North Atlantic (NA)	−10.2	−1.6	−0.34	−1.6
Indian Ocean (IO)	−6.7	−1.4	−0.08	−0.2
Global (GOGA)	−17.5	−2.7	−0.26	−0.9

Text S7. Linearity of the basin decomposition

We tested for additivity by comparing the linear sum of the single-basin responses (TP + NA + IO) with the global response (GOGA) and mapping the residual NL = GOGA − (TP + NA + IO) (Fig. 5 of the main text; Table S5). The sum overshot the global response by ~36% for 850 hPa geopotential height (−10.5 versus −7.7 m) and by ~40% for meridional wind, indicating saturation of the subtropical-high response as successive basins force it; however, the residual was not significant (Z850 NL = +2.8 m, $t \approx 0.9$); thus, the basin decomposition is equally consistent with additivity within the ensemble uncertainty.

Table S5: Linearity of the forced response over the Korea box: single-basin responses, their linear sum, global (GOGA) response, and residual (GOGA − sum) with its two-sample *t*-statistic.

Field	TP	NA	IO	Sum (TP + NA + IO)	GOGA	Residual (*t*)
Z850 (m)	−1.8	−3.7	−5.0	−10.5	−7.7	+2.8 (0.9)
V850 (m s^{-1})	−0.20	−0.20	−0.09	−0.49	−0.35	+0.14 (0.6)
MFC (mm d^{-1})	−0.32	−0.34	−0.08	−0.74	−0.26	+0.48 (1.0)

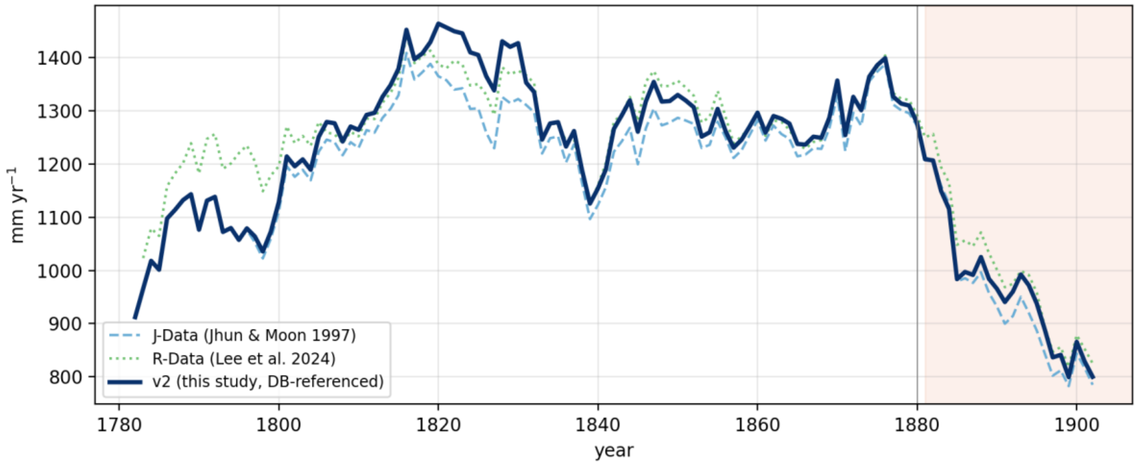

Figure S1: Annual precipitation from three independent reconstructions (11-year running mean): J-Data (Jhun and Moon, 1997), R-Data (Lee et al., 2024), and the reconciled v2 of this study, with reference to the NIKH database. The 1881–1907 drought (shaded) is essentially identical in all three, confirming its independence from reconstruction choice or amount reference.

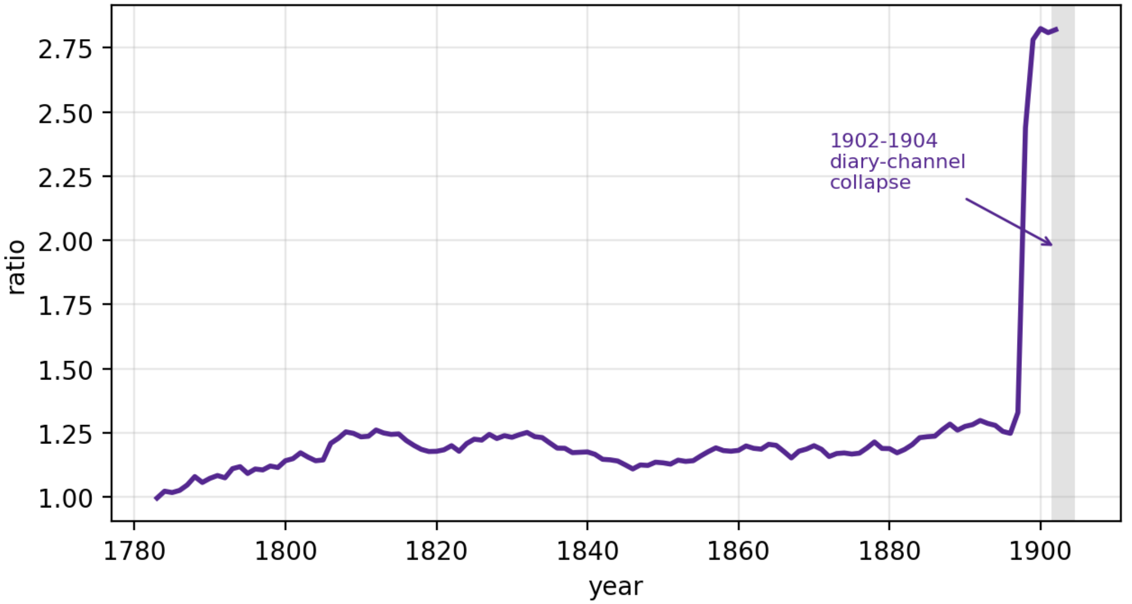

Figure S2: Ratio of measured (Cheugugi) to reported (Seungjeongwon Ilgi "rain") wet days over April–October (11-year running mean). In the annual data the ratio is stable from 1778 through 1901 – including the first two decades of the drought (annual values 0.9–1.5) – and spikes only in 1902–1904 (shaded band), when the qualitative diary channel briefly collapses (3–7 SJW rain-report days in 1903–1904); the smoothed curve begins to rise near 1897 only because the 11-year window spreads this spike backward. Record degradation therefore affected the diary channel two decades after the drought onset, not the gauge series during it. The three underlying channels are shown in Fig. 1d of the main text.

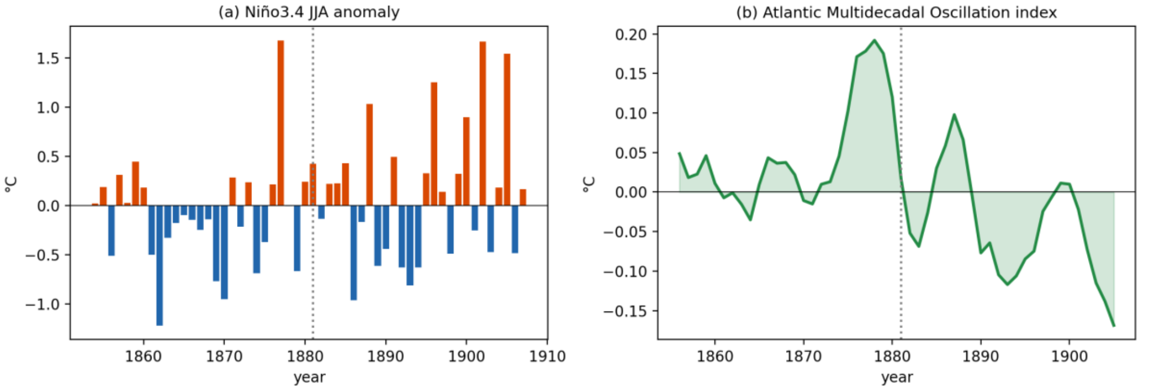

Figure S3: Ocean indices accompanying the drought. (a) JJA Niño3.4 anomaly (ERSSTv5); El Niño-like summers become more frequent after 1881 (dotted line), 19% versus 4% before. (b) Atlantic Multidecadal Oscillation index (5-year running mean) shifting to cold phase. These represent concurrent mean-state differences, not an established cause of the drought (see main text, Sect. 3.4).

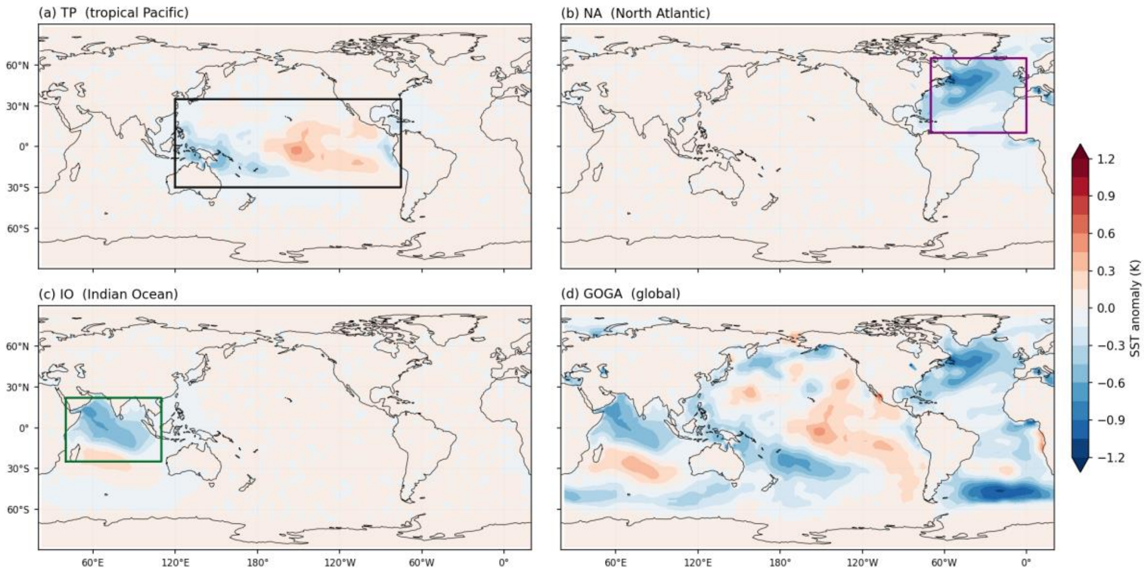

Figure S4: Prescribed JJA SST anomaly for each pacemaker experiment (1881–1907 minus 1855–1880, K) – the basin-masked ERSSTv5 anomaly added to the model climatology. (a) Tropical Pacific (TP), (b) North Atlantic (NA), (c) Indian Ocean (IO), and (d) global ocean (GOGA). Boxes outline the tanh-tapered basin masks (TP black, NA purple, IO green). Each single-basin experiment imposes the anomaly only within its box (tapering to zero outside). GOGA prescribes the entire observed pattern – an El Niño-like tropical Pacific set against a cooler North Atlantic and Indian Ocean (cf. Fig. 3b of the main text). These fields, imposed over 1854–1920, represent the boundary forcing, for which the Korean circulation response is attributed in Sect. 3.5.

References

Adler, R. F., Sapiano, M. R. P., Huffman, G. J., Wang, J.-J., Gu, G., Bolvin, D., Chiu, L., Schneider, U., Becker, A., Nelkin, E., Xie, P., Ferraro, R., and Shin, D.-B.: The Global Precipitation Climatology Project (GPCP) monthly analysis (new version 2.3) and a review of 2017 global precipitation, Atmosphere, 9, 138, https://doi.org/10.3390/atmos9040138, 2018.

Jhun, J.-G. and Moon, B.-K.: Restorations and analyses of rainfall amount observed by Chukwookee, J. Korean Meteorol. Soc., 33, 691–707, 1997.

Kalnay, E., Kanamitsu, M., Kistler, R., Collins, W., Deaven, D., Gandin, L., Iredell, M., Saha, S., White, G., Woollen, J., Zhu, Y., Leetmaa, A., Reynolds, R., Chelliah, M., Ebisuzaki, W., Higgins, W., Janowiak, J., Mo, K. C., Ropelewski, C., Wang, J., Jenne, R., and Joseph, D.: The NCEP/NCAR 40-year reanalysis project, B. Am. Meteorol. Soc., 77, 437–471, https://doi.org/10.1175/1520-0477(1996)077<0437:TNYRP>2.0.CO;2, 1996.

Kim, J.-K.: Parameterization of land surface processes in an atmospheric general circulation model, Ph.D. thesis, Seoul National University, Seoul, Republic of Korea, 1999 (in Korean).

Lee, J.-W., Shin, H.-J., and Hong, J.: Precipitation data in Seoul, Korea during 1778–1907, Sci. Data, 11, 566, https://doi.org/10.1038/s41597-024-03335-8, 2024.

Numaguti, A., Takahashi, M., Nakajima, T., and Sumi, A.: Description of CCSR/NIES atmospheric general circulation model, in: CGER's Supercomputer Monograph Report No. 3, Center for Global Environmental Research, National Institute for Environmental Studies, Tsukuba, Japan, 1–48, 1997.